

# Pyrazolylborate Nickel(II) Complexes as Catalysts for the Formation of Polyketones from Ethene and Carbon Monoxide – Partial Hydrolysis of the Bis(pyrazolyl)borate Yields a Pyrazolyl(hydroxo)borate Ligand

Wolfgang Kläui,<sup>\*,[a]</sup> Barbara Turkowski,<sup>[a]</sup> Gerd Rheinwald,<sup>[b]</sup> and Heinrich Lang<sup>[b]</sup>

**Keywords:** Nickel / N ligands / Homogeneous catalysis / Copolymerization / Polyketones / Solvolysis

The new nickel(II) complex  $[\text{Ni}\{\text{BBN}(\text{pz})_2\}(\text{o-tol})(\text{PPh}_3)]$  (**1**) of the bis(pyrazolyl)borate ligand  $[\text{BBN}(\text{pz})_2]^-$  (BBN = 1,5 borabicyclo[3.3.1]nonane) has been prepared by reaction of  $[\text{NiBr}(\text{o-tol})(\text{PPh}_3)_2]$  with  $\text{K}[\text{BBN}(\text{pz})_2]$ . In the presence of moisture this reaction yields the nickel(II) complex  $[\text{Ni}\{\text{BBN}(\text{pz})(\text{OH})\}(\text{o-tol})(\text{PPh}_3)]$  (**2**). The hydroxoborate ligand  $[\text{BBN}(\text{pz})(\text{OH})]^-$  acts as an *N,O*-chelate ligand in **2**.

Compound **1** and the analogous nickel complex  $[\text{Ni}\{\text{HB}(3\text{-Phpz})_3\}(\text{o-tol})(\text{PPh}_3)]$  show very similar activity in the catalytic copolymerization of carbon monoxide and ethene. This suggests that the borane hydrogen and the noncoordinated pyrazolyl ring in the latter are not essential for the catalysis. Compound **2** is inactive. Both **1** and **2** were characterised by X-ray crystallography.

## Introduction

Recently we have found that the nickel(II) complex  $[\text{Ni}\{\text{HB}(3\text{-Phpz})_3\}(\text{o-tol})(\text{PPh}_3)]$  catalyses the copolymerization of carbon monoxide and ethene under mild reaction conditions.<sup>[1]</sup> The coordination around nickel is planar with the tripodal tris(pyrazolyl)borate moiety acting as a bidentate ligand. In the solid state the third, noncoordinated pyrazolyl ring faces away from the coordination plane. This has the effect that borane hydrogen lies in the vicinity of nickel (Figure 1).

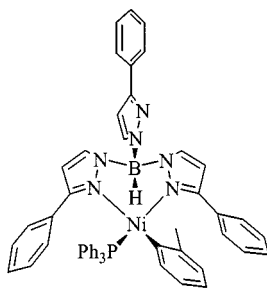
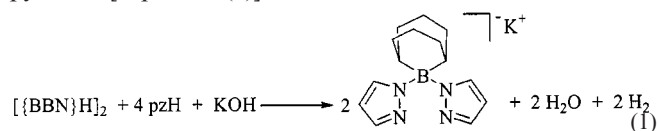


Figure 1. The structure of  $[\text{Ni}\{\text{HB}(3\text{-Phpz})_3\}(\text{o-tol})(\text{PPh}_3)]$

It was not clear at all why this nickel(II) complex is catalytically active. Does the tridenticity of the ligand play a role? Is the borane hydrogen important for the catalysis?

To answer these questions, we have now synthesised an analogous nickel(II) complex with the dipodal bis(pyrazolyl)borate ligand  $[\text{BBN}(\text{pz})_2]^-$ . The potassium salt of this ligand is accessible from BBN, potassium pyrazolide and pyrazole [Equation (1)].<sup>[2,3]</sup>



Herein we report the synthesis, crystal structure, and catalytic activity of the novel organonickel(II) complex  $[\text{Ni}\{\text{BBN}(\text{pz})_2\}(\text{o-tol})(\text{PPh}_3)]$  (**1**) (Figure 2).

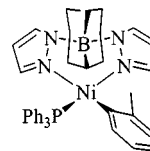


Figure 2. The structure of  $[\text{Ni}\{\text{BBN}(\text{pz})_2\}(\text{o-tol})(\text{PPh}_3)]$  (**1**)

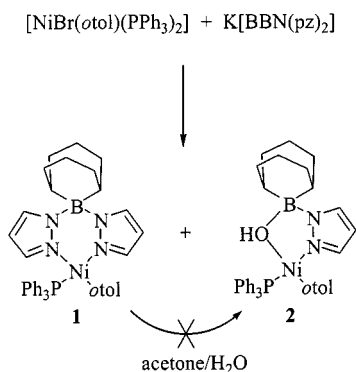
## Results and Discussion

### Synthesis of the Nickel(II) Complexes

$[\text{Ni}\{\text{BBN}(\text{pz})_2\}(\text{o-tol})(\text{PPh}_3)]$  (**1**) was prepared by reacting  $[\text{NiBr}(\text{o-tol})(\text{PPh}_3)_2]$  with  $\text{K}[\text{BBN}(\text{pz})_2]$  in THF (Scheme 1). In the presence of moisture the ligand  $[\text{BBN}(\text{pz})_2]^-$  partly hydrolyses to form a hydroxoborate. This in turn acts as an *N,O*-chelate ligand to give the unusual complex  $[\text{Ni}\{\text{BBN}(\text{pz})(\text{OH})\}(\text{o-tol})(\text{PPh}_3)]$  (**2**).

<sup>[a]</sup> Institut für Anorganische Chemie und Strukturchemie der Universität Düsseldorf, Universitätsstraße 1, 40225 Düsseldorf, Germany, Fax: (internat.) + 49-211/81-12287 E-mail: klaui@uni-duesseldorf.de

<sup>[b]</sup> Lehrstuhl für Anorganische Chemie, Technische Universität Chemnitz, Straße der Nationen 62, 09107 Chemnitz, Germany



Scheme 1. Synthesis of the nickel complexes  $[\text{Ni}\{\text{BBN}(\text{pz})_2\}(\text{o-tol})(\text{PPh}_3)]$  (**1**) and  $[\text{Ni}\{\text{BBN}(\text{pz})(\text{OH})\}(\text{o-tol})(\text{PPh}_3)]$  (**2**)

The  $^1\text{H}$  NMR spectra of **1** and **2** are similar and show the expected signals. The signals of the pyrazolyl ring and of the methyl group of the *o*-tolyl ligand in **2** experience a low-field shift in comparison with the ones of **1**. The BBN signals of both nickel complexes in the range  $\delta = 0.5\text{--}2.3$  are broad and unresolved. The signal shifted downfield to  $\delta = 4.4$  is assigned to the C7 proton, which is oriented towards the nickel atom (see Figure 3). A similar effect has been observed in the nickel complex  $[\text{Ni}\{\text{Et}_2\text{B}(\text{pz})_2\}_2]$ .<sup>[4]</sup> The signal of the hydroxyl proton in **2** appears as a doublet at  $\delta = -0.5$ . A  $^1\text{H}\{^{31}\text{P}\}$  NMR decoupling experiment shows that the doublet structure is due to a  $^3J_{\text{PH}}$  coupling.

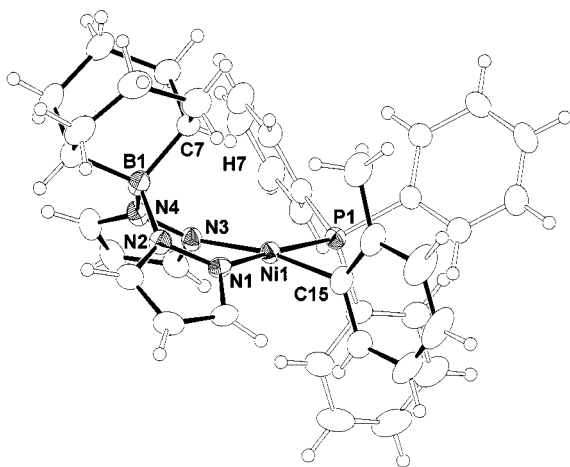
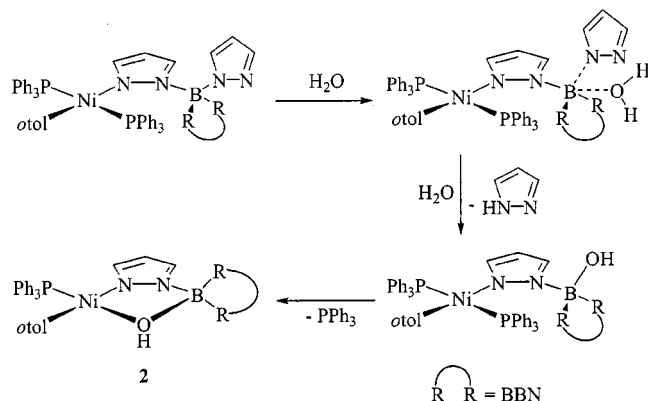


Figure 3. ZORTEP plot of  $[\text{Ni}\{\text{BBN}(\text{pz})_2\}(\text{o-tol})(\text{PPh}_3)]$  (**1**)

We have tried to pin down the conditions under which the hydroxoborate complex **2** is formed. From separate experiments we know that: (i) complex **1** does not hydrolyse to yield complex **2**, and (ii) the hydrolysis of the ligand  $[\text{BBN}(\text{pz})]^-$  in the absence of the nickel complex  $[\text{NiBr}(\text{o-tol})(\text{PPh}_3)_2]$  is much slower than the formation of **2**. In Scheme 2 we have postulated how the formation of **2** could occur.<sup>[5]</sup>



Scheme 2. Hydrolysis of the  $[\text{BBN}(\text{pz})_2]^-$  ligand during the synthesis of **2**

### Crystal Structures of the Nickel(II) Complexes

#### $[\text{Ni}\{\text{BBN}(\text{pz})_2\}(\text{o-tol})(\text{PPh}_3)]$ (**1**)

The nickel complex **1** crystallises from acetone as dark yellow plates [monoclinic space group  $Pn$  with  $a = 12.1313(8)$ ,  $b = 13.0085(8)$ ,  $c = 12.6192(8)$  Å, and  $\beta = 107.492(2)^\circ$ ]. The compound co-crystallizes with one molecule of acetone per formula unit. Figure 3 shows the structure of **1** in the crystal.

The four-coordinate nickel atom is in a planar arrangement. The bis(pyrazolyl)borate ligand coordinates in a bidentate fashion with a bite angle  $\text{N1}–\text{Ni1}–\text{N3}$  of  $89.80(13)^\circ$ , and forms a six-membered chelate ring in a boat conformation. The *o*-tolyl ring is orientated nearly perpendicular to the coordination plane [torsion angle  $\text{P1}–\text{Ni1}–\text{C15}–\text{C16}$ :  $99.2(4)^\circ$ ] in order to minimise the interaction with the neighbouring ligands.

The incorporated acetone molecule shows a weak non-classical hydrogen bond between H25 and the symmetry generated O1a (values are given in Table 1). The bond lengths and bond angles are in the expected<sup>[1]</sup> range (see Table 1).

#### $[\text{Ni}\{\text{BBN}(\text{pz})(\text{OH})\}(\text{o-tol})(\text{PPh}_3)]$ (**2**)

The nickel complex **2** crystallises from acetone as dark-yellow triclinic blocks [triclinic space group  $P\bar{1}$  with  $a = 12.1983(10)$ ,  $b = 12.3689(10)$ ,  $c = 13.7388(11)$  Å,  $\alpha = 112.086(2)$ ,  $\beta = 112.360(2)$  and  $\gamma = 90.462(2)^\circ$ ]. The compound co-crystallizes with one molecule of acetone per formula unit. Figure 4 shows the structure of **2** in the crystal.

The nickel atom is in a planar environment. The hydroxoborate ligand coordinates in a bidentate fashion with the nitrogen of the pyrazolyl ring and the oxygen of the hydroxyl group. The five-membered chelate ring shows an envelope conformation with a bite angle  $\text{N1}–\text{Ni1}–\text{O1}$  of  $81.5^\circ$ .

The deviations from the least-squares plane including the atoms N1, N2, B1, O1, and Ni1 are:  $0.0472(0.0008)$ ,  $0.0488(0.0010)$ ,  $-0.1612(0.0010)$ ,  $0.1836(0.0009)$  and  $-0.1184(0.0007)$  Å, respectively.

Table 1. Selected distances (Å) and angles (°) of **1**

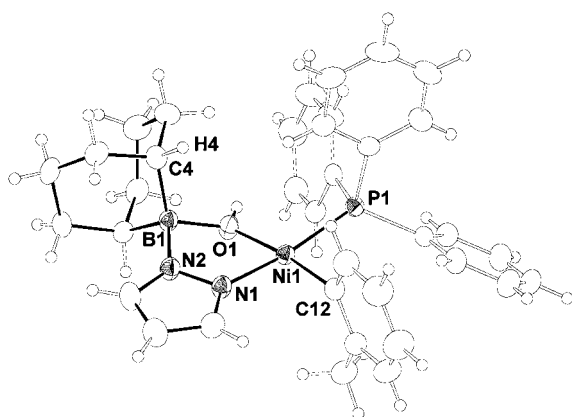
Ni1–C15	1.898(4)	C15–Ni1–N1	88.45(17)
Ni1–N1	1.967(3)	C15–Ni1–N3	170.27(18)
Ni1–N3	1.988(3)	N1–Ni1–N3	89.80(13)
Ni1–P1	2.1603(11)	C15–Ni1–P1	84.64(15)
N2–B1	1.575(7)	N1–Ni1–P1	172.99(9)
N4–B1	1.590(6)	N3–Ni1–P1	97.21(11)
H7...Ni1	2.569	N2–Ni1–Ni1	122.3(3)
		N1–N2–B1	120.4(3)
		N2–B1–N4	100.8(3)
		N3–N4–B1	118.8(3)
		N4–N3–Ni1	124.5(2)
C25–H25	0.95	C25–H25–O1a <sup>[a]</sup>	142.6
H25–O1a <sup>[a]</sup>	2.552		
C25–O1a <sup>[a]</sup>	3.356		

<sup>[a]</sup> Symmetry operation:  $a = -1/2 + x, 1 - y, -1/2 + z$ .

Table 2. Selected distances (Å) and angles (°) of **2**

Ni1–C12	1.8839(16)	C12–Ni1–O1	172.72(6)
Ni1–N1	1.8986(13)	N1–Ni1–O1	81.54(6)
Ni1–O1	1.9195(12)	C12–Ni1–P1	89.63(5)
Ni1–P1	2.1520(5)	C12–Ni1–N1	91.76(6)
O1–B1	1.590(6)	N1–Ni1–P1	171.27(4)
N2–B1	1.528(2)	O1–Ni1–P1	97.43(4)
H4...Ni	3.559	N2–Ni1–Ni1	116.56(10)
		N1–N2–B1	118.04(12)
		N2–B1–O1	97.83(12)
		B1–O1–Ni1	119.14(10)
C1–H1	0.916(19)	C1–H1–O2a <sup>[a]</sup>	153.48
H1–O2a <sup>[a]</sup>	2.4642		
C1–O2a <sup>[a]</sup>	3.3089		
C22–H22	0.98(2)	C22–H22–O2b <sup>[b]</sup>	162.98
H22–O2b <sup>[b]</sup>	2.4144		
C22–O2b <sup>[b]</sup>	3.3655		

<sup>[a]</sup> Symmetry operation:  $a = 2 - x, 1 - y, 1 - z$ . <sup>[b]</sup> Symmetry operation:  $b = 1 - x, 1 - y, 1 - z$ .

Figure 4. ORTEP plot of  $[\text{Ni}\{\text{BBN}(\text{pz})(\text{OH})\}(o\text{-tol})(\text{PPh}_3)]$  (**2**)

As in **1**, the incorporated acetone shows a weak nonclassical hydrogen bond between H1 and O2a as well as between H22 and O2b.

The bond lengths and bond angles are in the expected range.<sup>[1,6,7]</sup> Selected distances and angles of **2** are presented in Table 2.

### Copolymerization Reactions with $[\text{Ni}\{\text{BBN}(\text{pz})_2\}(o\text{-tol})(\text{PPh}_3)]$ (**1**)

The copolymerization of carbon monoxide and ethene was performed according to the reaction conditions reported for  $[\text{Ni}\{\text{HB}(3\text{-Phpz})_3\}(o\text{-tol})(\text{PPh}_3)]$  as catalyst.<sup>[1]</sup>

Table 3. Copolymerization of carbon monoxide and ethene at 60 °C in toluene; comparison of the nickel catalysts **1** and  $[\text{Ni}\{\text{HB}(3\text{-Phpz})_3\}(o\text{-tol})(\text{PPh}_3)]$ <sup>[1]</sup>

Catalyst	Ethene pressure (bar)	CO pressure (bar)	Polyketone (g)	Efficiency (gPK/gNi)
<b>1</b>	40	20	0.47	60
<b>1</b>	40	10	0.70	90
<b>1</b>	40	3.5	0.38	50
$[\text{Ni}\{\text{HB}(3\text{-Phpz})_3\}(o\text{-tol})(\text{PPh}_3)]$	40	2.0	0.23	34
$[\text{Ni}\{\text{HB}(3\text{-Phpz})_3\}(o\text{-tol})(\text{PPh}_3)]$	40	3.5	1.15	167
$[\text{Ni}\{\text{HB}(3\text{-Phpz})_3\}(o\text{-tol})(\text{PPh}_3)]$	40	5.0	0.31	45

## Experimental Section

**General Remarks:** All reactions were carried out under nitrogen using standard Schlenk techniques unless stated otherwise. All solvents were purified and degassed by standard procedures. THF for the synthesis of **2** was not dried. The compounds  $\text{K}[\text{BBN}(\text{pz})_2]$ <sup>[3]</sup> and  $[\text{NiBr}(o\text{-tol})(\text{PPh}_3)_2]$ <sup>[8]</sup> were synthesized according to literature procedures. Filtration was done with 1  $\mu\text{m}$  membrane filters (regenerated cellulose, Schleicher & Schuell). One dimensional  $^1\text{H}$  and  $^{31}\text{P}$  NMR spectra were recorded on a Bruker DRX 200 spectrometer at 296 K. The proton chemical shifts ( $\delta$ ) are given in ppm and referenced to the signal of partially deuterated  $\text{CDCl}_3$  at  $\delta = 7.3$ . The phosphorus chemical shifts are referenced to the signal of external  $\text{H}_3\text{PO}_4$ . Infrared spectra were recorded on a FT-IR Bruker IFS 66 spectrometer. EIMS data were recorded on a Varian MAT 311 A instrument, ionisation energy 70 eV. FAB mass spectra were recorded on a Finnigan MAT 8200 spectrometer using an NBA matrix. Elemental analyses were performed on a Perkin–Elmer CHN-2400/II elemental analyser.

**Preparation of the Nickel(II) Complexes 1 and 2:** A solution of  $[\text{NiBr}(o\text{-tol})(\text{PPh}_3)_2]$  (1.0 g, 1.3 mmol) and  $\text{K}[\text{BBN}(\text{pz})_2]$  (0.39 g, 1.3 mmol) in 25 mL of dry THF for **1** or in 25 mL of wet THF for **2** was stirred overnight. The solvent was evaporated, the residue was taken up in dichloromethane and filtered through a membrane filter. After evaporation of the solvent the residue was washed with about 10 mL of hexane. Crystallisation from diethyl ether (**1**) or acetone (**1** and **2**) yielded **1** and **2** as yellow crystals suitable for X-ray analysis.

**$[\text{Ni}\{\text{BBN}(\text{pz})_2\}(o\text{-tol})(\text{PPh}_3)]$  (**1**):** Yield: 0.51 g (57%).  $^1\text{H}$  NMR ( $\text{CDCl}_3$ ):  $\delta = 1.3\text{--}2.3$  (broad, 13 H, BBN), 2.3 (s, 3 H, *o*-tol  $\text{CH}_3$ ), 4.4 (s, 1 H, BBN), 5.7 (t, 1 H, pyrazolyl  $\text{C}^4\text{H}$ ), 5.9 (dt,  $^3J_{\text{H,H}} = 2$ ,  $^5J_{\text{P,H}} = 1$  Hz, 1 H, pyrazolyl  $\text{C}^4\text{H}$ ), 6.4 (dd,  $^3J_{\text{H,H}} = 7$ ,  $J = 2$  Hz, 1 H, *o*-tol), 6.6–6.7 (m, 2 H, *o*-tol), 6.8 (dd,  $^3J_{\text{H,H}} = 2$ ,  $^5J_{\text{P,H}} = 1$  Hz, 1 H, pyrazolyl  $\text{C}^{3/5}\text{H}$ ), 6.9 (d,  $^3J_{\text{H,H}} = 2$  Hz, 1 H, pyrazolyl  $\text{C}^{3/5}\text{H}$ ), 7.2–7.7 (m, 19 H,  $\text{PPh}_3$ , *o*-tol, pyrazolyl  $\text{C}^{3/5}\text{H}$ ).  $^{31}\text{P}\{^1\text{H}\}$  NMR ( $\text{CDCl}_3$ ):  $\delta = 29.5$ . IR (KBr):  $\tilde{\nu} = 2939\text{ cm}^{-1}$ , 2924, 2881, 2838 (m, C–H), 1499 (w, C=C), 1434, 1409 (m, P–C). MS

Table 4. Crystallographic data for  $[\text{Ni}\{\text{BBN}(\text{pz})_2\}(o\text{-tol})(\text{PPh}_3)]$  (**1**) and  $[\text{Ni}\{\text{BBN}(\text{pz})(\text{OH})\}(o\text{-tol})(\text{PPh}_3)]$  (**2**)

	<b>1</b>	<b>2</b>
Crystal shape	plate	triclinic block
Crystal colour	yellow	yellow
Crystal size ( $\text{mm}^3$ )	$0.5 \times 0.4 \times 0.08$	$0.46 \times 0.36 \times 0.18$
Chemical formula	$\text{C}_{36}\text{H}_{42}\text{BN}_4\text{NiP}\cdot\text{C}_3\text{H}_6\text{O}$	$\text{C}_{36}\text{H}_{40}\text{BN}_2\text{NiOP}\cdot\text{C}_3\text{H}_6\text{O}$
Molecular weight	725.33	675.27
Crystal system	Monoclinic	Triclinic
Space group	$Pn$	$P\bar{1}$
$a$ (Å)	12.1313(8)	12.1986(10)
$b$ (Å)	13.0085(8)	12.3689(10)
$c$ (Å)	12.6192(8)	13.7388(11)
$\alpha$ (°)	90	112.086(2)
$\beta$ (°)	107.492(2)	112.360(2)
$\gamma$ (°)	90	90.462(2)
Volume (Å <sup>3</sup> )	1889.3(2)	1748.5(2)
$Z$	2	2
$\rho$ (calcd., $\text{g/cm}^3$ )	1.268	1.283
Radiation used ( $\lambda$ , Å)	Mo- $K_\alpha$ (0.7173)	Mo- $K_\alpha$ (0.7173)
Temperature (K)	173(2)	173(2)
Scan method	$\omega$ scans	$\omega$ scans
Linear absorption coefficient ( $\text{mm}^{-1}$ )	0.591	0.637
Total reflections	8147	14631
Independent reflections	4348	9753
Unique reflections	3748	6793
Used reflections	4348	9753
$R(\text{int})$	0.0944	0.0246
$\theta$ -Scan range (°)	1.57 to 29.24	1.76 to 30.88
Index ranges	$-16 \leq h \leq 4$ $-17 \leq k \leq 17$ $-10 \leq l \leq 16$	$-17 \leq h \leq 13$ $-17 \leq k \leq 17$ $-18 \leq l \leq 19$
Completeness to $\theta_{\text{max}}$ (%)	75.2	88.5
$F(000)$	768	716
$R_{\text{[a]}}$	0.0423, 0.0931	0.0360, 0.0768
$wR^2 [I > 2\sigma(I)]^{\text{[b]}}$		
$R$ indices (all data), $wR^2$	0.0551, 0.0963	0.0635, 0.0840
Maximum $\delta/\sigma$	0.449	0.145
Max./min. e-density ( $\text{e}\cdot\text{\AA}^{-3}$ )	0.715/−0.740	0.411/−0.309
Used reflections	4348	9753
L. S. restraints	2	0
Refined parameters	454	599
Goodness-of-fit on $F^2$ $^{\text{[c]}}$	1.014	0.933
Weighting scheme parameters $a/b$ $^{\text{[d]}}$	0.0635/0	0.0414/0

$^{\text{[a]}}$   $R_1 = \Sigma(|F_o| - |F_c|)/\Sigma|F_o|$ .  $^{\text{[b]}}$   $wR^2 = [\Sigma(w(F_o^2 - F_c^2)^2)/\Sigma(wF_o^4)]^{1/2}$ .  $^{\text{[c]}}$   $S = [\Sigma w(F_o^2 - F_c^2)^2]/(n - p)^{1/2}$ ,  $n$  = number of reflections,  $p$  = parameters used.  $^{\text{[d]}}$  Definition of  $w$  calculation:  $w = 1/[\sigma^2(F_o^2) + (aP)^2 + bP]$  where  $P = (F_o^2 + 2F_c^2)/3$ .

(FAB<sup>+</sup>): *m/z* (%) = 665 (6) [M<sup>+</sup> – H], 589 (1) [M<sup>+</sup> – pzH], 574 (72) [M<sup>+</sup> – *o*-tol], 556 (8) [M<sup>+</sup> – BBN], 507 (9) [M<sup>+</sup> – (*o*-tol, pzH)], 353 (100) [PPh<sub>3</sub>(*o*-tol)]<sup>+</sup>. C<sub>39</sub>H<sub>42</sub>BN<sub>4</sub>NiP·C<sub>3</sub>H<sub>6</sub>O (725.34): calcd. C 69.55, H 6.67, N 7.72; found C 69.60, H 6.70, N 7.95.

[Ni{BBN(pz)(OH)}(*o*-tol)(PPh<sub>3</sub>)] (2): Yield: 0.31 g (38%). <sup>1</sup>H NMR (CDCl<sub>3</sub>): δ = –0.5 (d, <sup>3</sup>J<sub>P,H</sub> = 1 Hz, 1 H, OH), 0.5 (s (broad), 1 H, BBN), 0.6 (s (broad), 1 H, BBN), 0.8–2.2 (broad, 12 H, BBN), 2.7 (s, 3 H, *o*-tol CH<sub>3</sub>), 6.1 (dt, <sup>3</sup>J<sub>H,H</sub> = 2, <sup>5</sup>J<sub>P,H</sub> = 1 Hz, 1 H, pyrazolyl C<sup>4</sup> H), 6.2 (d, <sup>3</sup>J<sub>H,H</sub> = 2 Hz, 1 H, pyrazolyl C<sup>3/5</sup> H), 6.5–6.8 (m, 3 H, *o*-tol), 7.3 (dt, <sup>3</sup>J<sub>H,H</sub> = 8, *J* = 1 Hz, 1 H, *o*-tol), 7.3–7.6 (m, 15 H, PPh<sub>3</sub>), 7.7–7.8 (m, 1 H, pyrazolyl C<sup>3/5</sup> H). <sup>31</sup>P{<sup>1</sup>H} NMR (CDCl<sub>3</sub>): δ = 30.6. IR (KBr):  $\tilde{\nu}$  = 3630 cm<sup>–1</sup> (s, sharp, O–H), 3043, 2978, 2936 (m, C–H), 2914 (s, C–H), 2863 (vs, C–H), 1497 (w, C=C), 1434 (s, P–C), 1404 (m, P–C). MS (EI, 220 °C): *m/z* (%) = 616 (3) [M<sup>+</sup>], 550 (<1) [M<sup>+</sup> – pz], 524 (3) [M<sup>+</sup> – *o*-tol], 354 (20) [PPh<sub>3</sub>(*o*-tol)]<sup>+</sup>, 262 (100) [PPh<sub>3</sub>]<sup>+</sup>. C<sub>36</sub>H<sub>40</sub>BN<sub>2</sub>NiOP·C<sub>3</sub>H<sub>6</sub>O (675.28): calcd. C 69.37, H 6.87, N 4.15; found C 69.31, H 6.85, N 4.27.

**General Preparation for the Synthesis of Polyketone:** Compound 1 (0.12 mmol, 0.086 g) in 10 mL of toluene was transferred into a 100 mL autoclave. The solution was pressurised with carbon monoxide and then with ethene and stirred with a magnetic stirrer at 60 °C for 16 h. The white solid was filtered off, washed with hexane, and dried (see Table 3).

**Crystal Structure Analysis:** For compounds 1 and 2 data collection was carried out using a CCD area detector SMART 1 K by Bruker AXS GmbH with graphite monochromated Mo-*K*<sub>α</sub> radiation (λ = 0.71073 Å). Data collection was done at 173 K. For protection against oxygen or moisture, the preparation of single crystals was done in a perfluoroalkyl ether from ABCR GmbH & Co KG (viscosity 1600 cSt). The unit cell was determined with the program SMART.<sup>[9]</sup> For data integration and refinement of the unit cell the program SAINT<sup>[9]</sup> was used. The space group was determined using the programs XPREP<sup>[9]</sup> (1) and ABSEN<sup>[10]</sup> (2) and the empirical absorption correction was done with SADABS.<sup>[9]</sup> The structures were solved by direct methods using the programs SHELX-97<sup>[11]</sup> for (1) and SIR97<sup>[12]</sup> for (2), the structure refinement was based on least-squares methods based on *F*<sup>2</sup> with SHELX-97.<sup>[11]</sup> The plots of the molecular structures were visualised using the program ZORTEP.<sup>[13]</sup>

All non-hydrogen atoms were fully refined in the calculated positions. For 2 the hydrogen atoms were taken from the electron density difference map and refined freely. For 1 the hydrogen atoms were positioned as riding on their neighbouring atoms and refined depending on its position. The figure in parenthesis after each calculated value represents the standard deviation in units of the last significant digit. Crystal data and refinement parameters are summarized in Table 4.

Crystallographic data (excluding structure factors) for the structures reported in this paper have been deposited with the Cambridge Crystallographic Data Centre as supplementary publication no. CCDC-165852 (1) and 165853 (2). Copies of the data can be obtained free of charge on application to CCDC, 12 Union Road, Cambridge CB2 1EZ, UK [Fax: (internat.) + 44(1223)336–033; E-mail: deposit@ccdc.cam.ac.uk].

- [1] B. Domhöver, W. Kläui, R. Bell, D. Motz, *Angew. Chem.* **1998**, *110*, 3218–3220; *Angew. Chem. Int. Ed.* **1998**, *37*, 3050–3052.
- [2] S. Trofimenko, J. C. Calabrese, J. S. Thompson, *Angew. Chem.* **1989**, *101*, 207–208; *Angew. Chem. Int. Ed.* **1989**, *28*, 205–206.
- [3] M. Bortolini, U. E. Bucher, H. Rüegger, L. M. Venanzi, *Organometallics* **1992**, *11*, 2514–2521.
- [4] S. Trofimenko, *J. Am. Chem. Soc.* **1967**, *89*, 6288–6294.
- [5] This reaction has been formulated in analogy to a similar reaction which has been observed by Macchioni et al.: G. Bellachioni, G. Cardaci, V. Gramlich, A. Macchioni, F. Pieroni, L. M. Venanzi, *J. Chem. Soc., Dalton Trans.* **1998**, 947–951.
- [6] W. Kläui, J. Bongards, G. J. Reiß, *Angew. Chem.* **2000**, *112*, 4077–4079; *Angew. Chem. Int. Ed.* **2000**, *39*, 3894–3896.
- [7] A. Y. Desjardins, K. J. Cavell, J. L. Hoare, B. W. Skelton, A. N. Sobolev, A. H. White, W. Keim, *J. Organomet. Chem.* **1997**, *544*, 163–174.
- [8] M. Hidai, T. Kashiwagi, T. Ikeuchi, Y. Uchida, *J. Organomet. Chem.* **1971**, *30*, 279–284.
- [9] Bruker AXS Inc., Madison, WI, USA, **1998**.
- [10] P. McArdle, *J. Appl. Cryst.* **1996**, *29*, 306.
- [11] G. M. Sheldrick, SHELX-97, Programs for Crystal Structure Analysis (Release 97-2), University of Göttingen, Germany **1997**.
- [12] A. Altomare, M. C. Burla, M. Camalli, G. L. Cascarano, C. Giacovazzo, A. Guagliardi, A. G. G. Moliterni, G. Polidori, R. Spagna, *J. Appl. Cryst.* **1999**, *32*, 115–119.
- [13] L. Zsolnai, G. Huttner, University of Heidelberg, Germany, **1994**.

Received June 27, 2001

[I01237]